AD-A170 257 STRESS AND DEFORMATION ANALYSIS OF AUTOFRETTAGED HIGH PRESSURE VESSELS(U) ARMY CLOSE COMBAT ARMAMENTS CENTER WATERVLIET NY P C CHEN JUN 86 ARCCB-TR-86020 1/1

UNCLASSIFIED F/G 13/13 NL

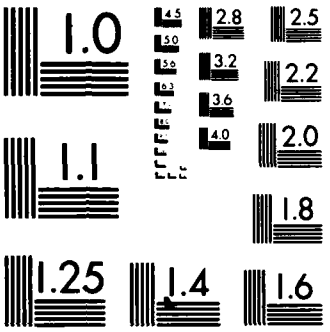

(12)

AD

TECHNICAL REPORT ARCCB-TR-86020

# STRESS AND DEFORMATION ANALYSIS OF AUTOFRETTAGED HIGH PRESSURE VESSELS



P. C. T. CHEN



JUNE 1986

US ARMY ARMAMENT RESEARCH AND DEVELOPMENT CENTER
CLOSE COMBAT ARMAMENTS CENTER
BENET WEAPONS LABORATORY
WATERVLIET, N.Y. 12189-4050



APPROVED FOR PUBLIC RELEASE; DISTRIBUTION UNLIMITED

## DISCLAIMER

The findings in this report are not to be construed as an official Department of the Army position unless so designated by other authorized documents.

The use of trade name(s) and/or manufacturer(s) does not constitute an official indorsement or approval.

## DESTRUCTION NOTICE

For classified documents, follow the procedures in DoD 5200.22-M, Industrial Security Manual, Section II-19 or DoD 5200.1-R, Information Security Program Regulation, Chapter IX.

For unclassified, limited documents, destroy by any method that will prevent disclosure of contents or reconstruction of the document.

For unclassified, unlimited documents, destroy when the report is no longer needed. Do not return it to the originator.

SECURITY CLASSIFICATION OF THIS PAGE *(When Data Entered)*

| REPORT DOCUMENTATION PAGE | READ INSTRUCTIONS BEFORE COMPLETING FORM |
|---|---|
| 1. REPORT NUMBER<br>ARCCB-TR-86020 | 2. GOVT ACCESSION NO.<br>AD-A170257 | 3. RECIPIENT'S CATALOG NUMBER |
| 4. TITLE *(and Subtitle)*<br>STRESS AND DEFORMATION ANALYSIS OF AUTOFRETTAGED HIGH PRESSURE VESSELS | | 5. TYPE OF REPORT & PERIOD COVERED<br>Final<br>6. PERFORMING ORG. REPORT NUMBER |
| 7. AUTHOR(s)<br>P. C. T. Chen | | 8. CONTRACT OR GRANT NUMBER(s) |
| 9. PERFORMING ORGANIZATION NAME AND ADDRESS<br>US Army Armament Research, Develop, & Engr Center<br>Benet Weapons Laboratory, SMCAR-CCB-TL<br>Watervliet, NY 12189-4050 | | 10. PROGRAM ELEMENT, PROJECT, TASK AREA & WORK UNIT NUMBERS<br>AMCMS No. 6111.02.H600.0<br>PRON No. 1A6DZ602NMSC |
| 11. CONTROLLING OFFICE NAME AND ADDRESS<br>US Army Armament Research, Develop, & Engr Center<br>Close Combat Armaments Center<br>Dover, NJ 07801-5001 | | 12. REPORT DATE<br>June 1986<br>13. NUMBER OF PAGES<br>20 |
| 14. MONITORING AGENCY NAME & ADDRESS(if different from Controlling Office) | | 15. SECURITY CLASS. (of this report)<br>UNCLASSIFIED<br>15a. DECLASSIFICATION/DOWNGRADING SCHEDULE |

16. DISTRIBUTION STATEMENT *(of this Report)*

Approved for public release; distribution unlimited.

17. DISTRIBUTION STATEMENT *(of the abstract entered in Block 20, if different from Report)*

18. SUPPLEMENTARY NOTES

To be presented at ASME 1986 Pressure Vessel and Piping Conference, Chicago, IL, 21-26 July 1986.
To be published in Proceedings of the Conference.

19. KEY WORDS *(Continue on reverse side if necessary and identify by block number)*

| | |
|---|---|
| High Strength Steel | Strain Hardening |
| Pressure Vessel | Residual Stress |
| Bauschinger Effect | Autofrettage |

20. ABSTRACT *(Continue on reverse side if necessary and identify by block number)*

A method of stress and deformation analysis based on a new theoretical model is reported. The new model is a close representation of the actual loading/unloading behavior in a high strength steel. The Bauschinger effect factor is treated as a function of overstrain. The strain-hardening effect is taken into account with different parameters used for loading and unloading processes. The formulas for calculating stresses, strains, and displacements are given and new results of residual stresses in autofrettaged high pressure vessels are presented.

DD FORM 1 JAN 73 1473 EDITION OF 1 NOV 65 IS OBSOLETE

UNCLASSIFIED

SECURITY CLASSIFICATION OF THIS PAGE *(When Data Entered)*

TABLE OF CONTENTS


| | Page |
|---|---|
| INTRODUCTION | 1 |
| MATERIAL BEHAVIOR AND MODELING | 2 |
| ELASTIC-PLASTIC LOADING | 5 |
| REVERSE YIELDING | 6 |
| ELASTIC-PLASTIC UNLOADING | 7 |
| NUMERICAL RESULTS AND DISCUSSION | 10 |
| REFERENCES | 18 |


LIST OF ILLUSTRATIONS


1. Stress-strain curve during loading and unloading. 4
2. Bauschinger effect factor as a function of overstrain. 5
3. Internal pressure and residual displacement vs. elastic-plastic interface for the case of wall ratio two. 11
4. Internal pressure and residual displacement vs. elastic-plastic interface for the case of wall ratio three. 12
5. Residual stress distribution in an autofrettaged tube (b/a = 2.0). 13
6. Residual stress distribution in an autofrettaged tube (b = 3a). 14
7. A comparison of residual stress based on three material models (b/a = 2, $\rho$/a = 1.75). 15
8. A comparison of residual stress based on three material models (b/a = 3, $\rho$/a = 2.0). 16
9. A comparison of residual stress based on three material models (b/a = 3, $\rho$/a = 3.0). 17

## INTRODUCTION

A thick-walled cylinder is used for a variety of applications in the chemical, nuclear, and armament industries where large internal pressures have to be withstood. In the absence of residual stresses, the cracks usually form at the bore where the hoop stress developed by the pressure is highest. To prevent such failure and to increase the pressure-carrying capacity, a common practice is autofrettage treatment of the cylinder prior to use (ref 1). This process has the effect of producing beneficial compressive residual hoop stresses near the bore which can prolong the fatigue life.

The determination of residual stresses in autofrettaged cylinders has been considered by many investigators using different mathematical methods and material models (refs 2-8). Most of the earlier solutions were based on the assumption that the material behaves elastically on the release of the autofrettage pressure. However, many materials, particularly the quenched and tempered, low alloy steels generally used for high pressure vessels, exhibit a significant Bauschinger effect (ref 9). In a recent paper (ref 10), this author presented a closed-form solution of residual stresses in autofrettaged tubes based on a theoretical model considering the Bauschinger and hardening effects during unloading, but neglecting the strain-hardening effects during loading. A more general theoretical model without this restriction was proposed earlier, but only part of the final results were shown due to space limitation (ref 11). In the present report, the complete method of stress and deformation analysis based on the general theoretical model is stated. The new model is a better representation of the actual loading/unloading behavior

---

References are listed at the end of this report.

in a high strength steel. The Bauschinger effect factor is treated as a function of overstrain. The strain-hardening effect is taken into account with different parameters used for loading and unloading processes. The formulas for calculating stresses, strains, and displacements are given and new results of residual stresses in autofrettaged high pressure vessels are presented.

## MATERIAL BEHAVIOR AND MODELING

The material chosen for this investigation was a modified 4330 steel having a martensitic structure. A description of its chemical composition and various heat treatments is given in Reference 9 by Milligan, Koo, and Davidson. They studied the material behavior by utilizing a uniaxial tension-compression specimen. Figure 1 shows the stress-strain curve during loading and unloading after overstrains in tension. The stress-strain curve during loading can be replaced with sufficient accuracy by a bilinear elastic-plastic model shown in the figure by the broken lines. For the plastic portion, the yield stress ($\sigma$) is related to the plastic strain ($\epsilon^p$) by

$$\sigma/\sigma_o = 1 + m\zeta/(1-m) \quad \text{and} \quad \zeta = (E/\sigma_o)\epsilon^p \tag{1}$$

where Young's modulus (E), tangent modulus (mE), initial yield stress ($\sigma_o$), and the Poisson's ratio ($\nu$) are the material constants. The nominal yield strength at 0.1 percent offset was chosen as the initial yield stress.

Initially, the yield stresses in tension and compression are approximately equal so that the material can be considered as isotropic. However, the ratio of the yield stress upon reverse yielding to the initial yield stress is strongly affected by overstrain in a high strength steel. The values of the Bauschinger effect factor (BEF) also depend on the 0.1 percent offset mentioned above. Taking into account strain-hardening, the definition of the BEF is

$$BEF = (\sigma_o'-\sigma_1)/\sigma_1 = f(\epsilon_1^p) \quad (2)$$

where $\sigma_1$, $\epsilon_1^p$ are the yield stress, plastic strain just before unloading occurs, and $\sigma_o'$ is the linear drop in stress until reverse yielding begins. Figure 2 shows the Bauschinger effect factor (f) as a function of percent tensile overstrain ($\epsilon^p$). The graph shows a decrease of the BEF with increasing amount of tensile prestrain up to approximately two percent at which point it becomes effectively constant.

In most of the plasticity theories, the curve of reverse loading is uniquely defined by the curve of the first loading. The present model does not assume such a relationship. The experimental stress-strain curve during unloading is used directly. A piecewise linear representation can be used, but only a bilinear approximation was chosen here as shown in Figure 1. In the same figure, we also show two other theoretical models in dotted lines for this material subjected to unloading with further plastic flow. They are isotropic and kinematic hardening models. A summary of the plasticity theories given by Armen (ref 12) illustrates the fact that all of the theories are capable of treating the monotonic loading situation. For cyclic loading, including reverse yielding, kinematic and isotropic hardening represent the limits to the actual behavior, whereas the remaining theories are falling anywhere within these limits. The above conclusion indicates that none of the existing models can accurately represent the actual material behavior as shown in Figure 1. The reverse yielding begins at a stress whose magnitude is smaller than that predicted by all existing theories and the slope of strain-hardening after reverse yielding is much larger than that during the first loading process. The new bilinear model presented here is a better approximation to the actual material behavior.

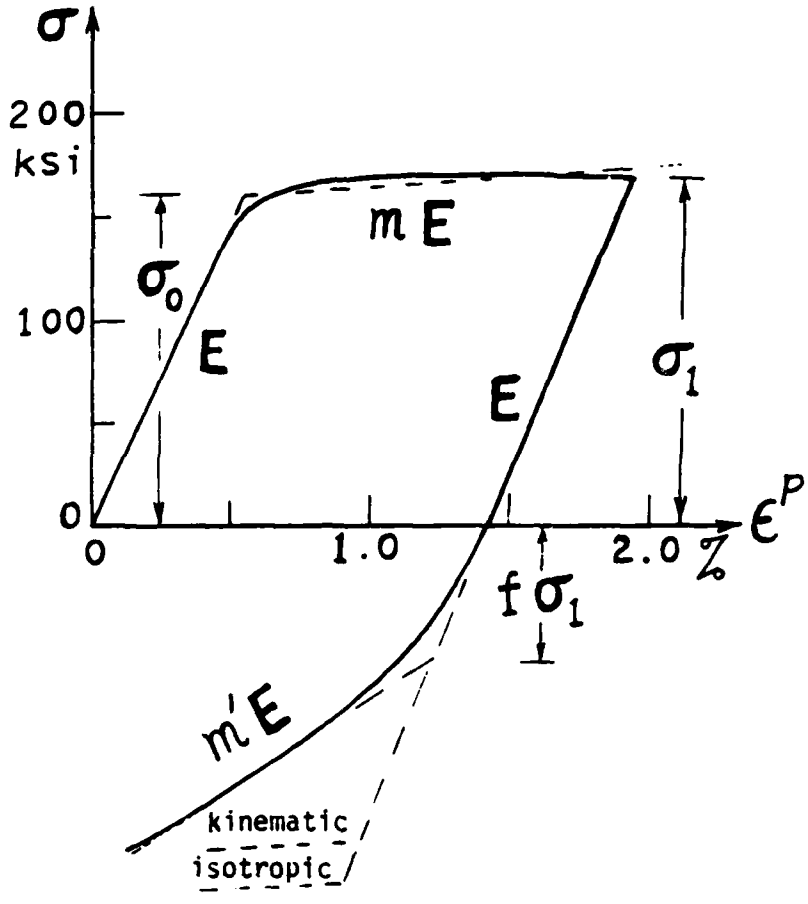


Figure 1. Stress-strain curve during loading and unloading.

Choosing a new coordinate system $(\sigma',\epsilon')$ with the origin at the point before unloading, we have for the plastic portion of the reverse yielding curve

$$\sigma'/\sigma_o = \sigma_o'/\sigma_o + m'\zeta'/(1-m') \quad \text{and} \quad \zeta' = (E/\sigma_o)\epsilon'^p \tag{3}$$

where $m'E$ is the slope of the reverse yielding curve and $\epsilon'^p$ is the additional plastic strain during unloading. According to Eqs. (1) and (2), $\sigma_o'$ can be expressed as a function of plastic strain $(\epsilon_1^p)$ just prior to unloading by

$$\sigma_o'/\sigma_o = [1 + m\zeta_1/(1-m)][1 + f(\zeta_1)] = g(\zeta_1) \tag{4}$$

With experimental data $f(\epsilon^p)$ shown in Figure 2, we can calculate $\sigma_o'$ and determine the initiation of reverse yielding. The slope of reverse yielding

(m'E) could be expressed also as a function of prestrain ($\epsilon^p$ and $\epsilon'^p$) if more experimental unloading curves were available. Based on limited information, the slope of reverse yielding (m'E) is estimated to be in the range of (9.4 to 8.3) x $10^6$ psi. It seems that this slope is not very sensitive to prestrain and a constant value, say m' = 0.3 may be assumed.

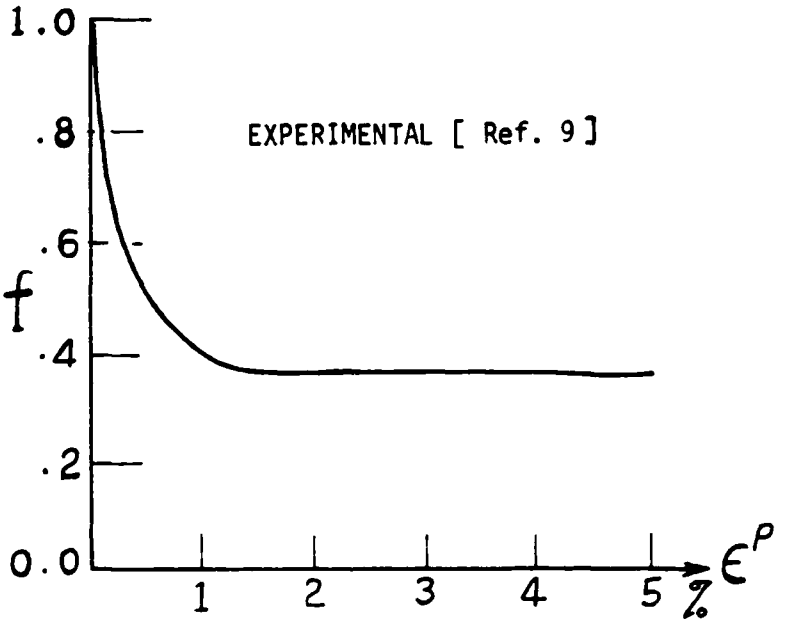


Figure 2. Bauschinger effect factor as a function of overstrain.

ELASTIC-PLASTIC LOADING

Consider a thick-walled cylinder, internal radius a and external radius b, which is subjected to internal pressure p. The material is assumed to be elastic-plastic, obeying the Tresca's yield criterion, the associated flow theory, and a linear strain-hardening rule. The elastic-plastic solution during loading has been found by Bland (ref 3). The expressions for the radial and hoop stresses are:

$$\frac{\sigma_r}{\sigma_o} = \frac{1}{2}\left(\mp 1 + \frac{\rho^2}{b^2}\right) \mp \frac{1}{2}\beta_2\left(\frac{\rho^2}{r^2} - 1\right) - (1-\beta_2)\log\frac{\rho}{r} \quad \text{for } a \leq r \leq \rho \tag{5}$$

$$\frac{\sigma_\theta}{\sigma_o} \tag{6}$$

subject to $\sigma_\theta \geq \sigma_z \geq \sigma_r$

$$\begin{matrix}\sigma_r/\sigma_o \\ \sigma_\theta/\sigma_o\end{matrix} = \frac{1}{2}\left(\frac{\rho^2}{b^2} \mp \frac{\rho^2}{r^2}\right) \quad \text{for } \rho \leq r \leq b \qquad \begin{matrix}(7) \\ (8)\end{matrix}$$

$$\sigma_z/\sigma_o = \nu(\sigma_r+\sigma_\theta)/\sigma_o + E\epsilon_z/\sigma_o \qquad (9)$$

$$\frac{E}{\sigma_o}\frac{u}{r} = (1-2\nu)(1+\nu)\frac{\sigma_r}{\sigma_o} + (1-\nu^2)\frac{\rho^2}{r^2} - \nu\frac{E}{\sigma_o}\epsilon_z \qquad (10)$$

and

$$(E/\sigma_o)\epsilon_z = \frac{(\mu-2\nu)}{b^2/a^2-1}(P/\sigma_o) \qquad (11)$$

where $\mu = 0$ (open-end), 1 (closed-end), and $\rho$ is the elastic-plastic boundary relating to the internal pressure p by

$$p/\sigma_o = \frac{1}{2}(1-\rho^2/b^2) + (1-\beta_2)\log(\rho/a) + \frac{1}{2}\beta_2(\rho^2/a^2-1) \qquad (12)$$

The equivalent plastic strain can be calculated by

$$(E/\sigma_o)\epsilon^p = \zeta = \beta_1(\rho^2/r^2-1) \quad , \quad \text{in } (a \leq r \leq \rho) \qquad (13)$$

and

$$\beta_1 = \frac{1-m}{m + \frac{\sqrt{3}}{2}\frac{(1-m)}{(1-\nu^2)}} \quad , \quad \beta_2 = m\beta_1/(1-m) \qquad (14)$$

## REVERSE YIELDING

If the pressure p given by Eq. (12) is subsequently removed completely with no reverse yielding, the unloading is entirely elastic and the solution is given by

$$\begin{matrix}\sigma_r' \\ \sigma_\theta'\end{matrix} = \frac{p}{b^2/a^2-1}\left[\pm\frac{b^2}{r^2} - 1\right] \qquad \begin{matrix}(15) \\ (16)\end{matrix}$$

$$\sigma_z' = \nu(\sigma_r'+\sigma_\theta') + E\,\epsilon_z' \qquad (17)$$

$$E\epsilon_z' = -(\mu-2\nu)p/(b^2/a^2-1) \qquad (18)$$

$$Eu'/r = -[(1-\nu-\mu\nu) + (1+\nu)b^2/r^2]p/(b^2/a^2-1) \tag{19}$$

Let a double prime denote a component in the residual state, i.e., $\sigma_\theta" = \sigma_\theta + \sigma_\theta'$. Assuming a reduced compressive yield strength as a result of the Bauschinger effect and using Tresca's yield criterion subject to $\sigma_r" > \sigma_z" > \sigma_\theta"$, the reverse yielding will not occur if

$$\sigma_r" - \sigma_\theta" \leq \sigma" = f\sigma_o[1 + m\zeta/(1-m)] \tag{20}$$

Substituting the loading and unloading solutions into Eq. (20), we can determine the minimum pressure ($p_m$) for reverse yielding to occur. The equation for $p_m$ is given by

$$p_m/\sigma_o = \frac{1}{2}(1-a^2/b^2)[1 + m\zeta_m/(1-m)][1 + f(\zeta_m)] \tag{21}$$

and $\zeta_m = \beta_1(\rho_m^2/a^2-1)$.

Equating Eq. (12) to (21), we can determine the minimum amount of overstrain ($\rho_m$) and calculate the minimum pressure ($p_m$) required for reverse yielding.

## ELASTIC-PLASTIC UNLOADING

Now suppose that the loading has been such that the internal pressure is larger than $p_m$ given by Eq. (21). On unloading, yielding will occur for $a \leq r \leq \rho'$ with $\rho' < \rho$. In the reverse yielding zone, the stresses in the residual state satisfy

$$\sigma_r" - \sigma_\theta" = \sigma" \tag{22}$$

assuming that $\sigma_r" \geq \sigma_z" \geq \sigma_\theta"$. Since the yield criterion during loading is

$$\sigma_\theta - \sigma_r = \sigma \tag{23}$$

we have

$$\sigma_r' - \sigma_\theta' \equiv (\sigma_r"-\sigma_\theta") + (\sigma_\theta-\sigma_r) = \sigma" + \sigma = \sigma' \tag{24}$$

where $\sigma$ and $\sigma'$ are defined by Eqs. (1) and (3), respectively.

The associated flow rule states that

$$d\epsilon_\theta'^p = -d\epsilon_r'^p \leq 0 \quad \text{and} \quad d\epsilon_z'^p = 0 \tag{25}$$

Therefore, we have

$$\epsilon_z' = \epsilon_z'^p = -\epsilon_z \tag{26}$$

Since $\epsilon_z'$ is now known, Hooke's law and equation of equilibrium

$$\sigma_\theta' = \sigma_r' + r\,(d\sigma_r'/dr) \tag{27}$$

can be used to express $\sigma_z'$ in terms of $\sigma_r'$

$$\sigma_z' = E\epsilon_z' + 2\nu\sigma_r' + \nu r(d\sigma_r'/dr) \tag{28}$$

Since the dilation is purely elastic,

$$du'/dr + u'/r + \epsilon_z' = E^{-1}(1-2\nu)(\sigma_r'+\sigma_\theta'+\sigma_z')$$

Integrating the above equation after substituting from Eqs. (27) and (28), we have

$$ru' = E^{-1}(1-2\nu)(1+\nu)r^2\sigma_r' - \nu\epsilon_z'r^2 + c' \tag{29}$$

where $c'$ is a constant. Now the strain components $\epsilon_\theta'$, $\epsilon_r'$, $\epsilon_\theta'^e$, $\epsilon_r'^e$ can all be expressed in terms of $\epsilon_z'$, $\sigma_r'$, and $d\sigma'/dr$.

Since $\epsilon_\theta'^p = \epsilon_\theta' - \epsilon_\theta'^e$, the plastic strain components are

$$\epsilon_\theta'^p = -\epsilon_r'^p = -E^{-1}(1-\nu^2)r(d\sigma_r'/dr) + c'/r^2 \tag{30}$$

and the equivalent plastic strain is

$$\epsilon'^p = \frac{-2}{\sqrt{3}}\,\epsilon_\theta'^p = \frac{-2}{\sqrt{3}}\,[c'/r^2 - E^{-1}(1-\nu^2)r d\sigma r'/dr] \tag{31}$$

it has been assumed that the sign of $d\epsilon_\theta'^p$ is the same throughout the unloading process and that it is negative. This will be the case when the internal pressure is removed during the unloading. In the plastic region, $a \leq r \leq \rho'$, we have

$$rd\sigma_r'/dr = \sigma_\theta' - \sigma_r' = \sigma' \tag{32}$$

Substituting Eq. (32) into Eq. (31), we can determine the constant c' by the condition that $\epsilon'^p = 0$ in the elastic region, $\rho' \leq r \leq b$, and obtain

$$\epsilon'^p = \frac{2}{\sqrt{3}} E^{-1}(1-\nu^2)[(\rho'^2/r^2)\sigma_o'\Big|_{\rho'} - \sigma'] \tag{33}$$

With the aid of Eqs. (3) and (4), we can simplify the above expression to the following form:

$$\zeta' = \beta_1[g(\zeta_{\rho'})\rho'^2/r^2 - g(\zeta)] \tag{34}$$

where $g(\zeta_{\rho'})$ is the value of $g(\zeta)$ given by Eq. (4) evaluated at $r = \rho'$ and

$$\beta_1' = (1-m')/[m' + \frac{\sqrt{3}}{2}\frac{(1-m')}{(1-\nu^2)}] \tag{35}$$

Equations (32) and (33) together with Eq. (3) suffice to determine $\sigma_r'$ in the plastic region. Integrating Eq. (32) with the boundary conditions that $\sigma_r'$ is continuous at $r = \rho'$ and $\sigma_r' = p$ at $r = a$, we have

$$\sigma_r'/\sigma_o = P/\sigma_o - \Gamma(\zeta_r,\zeta_a) \tag{36}$$

and

$$\sigma_r'/\sigma_o\Big|_{\rho'_+} = P/\sigma_o - \Gamma(\zeta_{\rho'},\zeta_a) \tag{37}$$

where

$$\Gamma(\zeta_r,\zeta_a) = -\frac{1}{2}(\beta_2'/\beta_1)(\rho'/\rho)^2(\zeta_r-\zeta_a)g(\zeta_{\rho'}) + (1-\beta_2')G(\zeta_r,\zeta_a) \tag{38}$$

$$G(\zeta_r,\zeta_a) = \int_{\zeta_r}^{\zeta_a} \frac{1}{2}(\zeta+\beta_1)^{-1}g(\zeta)d\zeta \tag{39}$$

$$\beta_2' = m'\beta_1'/(1-m') \quad , \quad g(\zeta) \text{ is given by Eq. (4)} \tag{40}$$

and $\zeta_r$, $\zeta_a$ can be calculated by Eq. (12). For some special cases, e.g. Reference 10, explicit expressions for $G(\zeta_r,\zeta_a)$ can be obtained. In general, numerical integration is needed.

The stresses in the elastic zone ($\rho' \leq r \leq b$) are

$$\sigma_r'/\sigma_o = \frac{1}{2} g(\zeta_\rho')[\pm(\rho'/r)^2 - (\rho'/b)^2] \quad (41)$$

$$\sigma_\theta'/\sigma_o \quad (42)$$

The other expressions in the entire tube ($a \leq r \leq b$) are

$$\sigma_z'/\sigma_o = \nu(\sigma_r'+\sigma_\theta')/\sigma_o + E\epsilon_z'/\sigma_o \quad (43)$$

$$E\epsilon_z'/\sigma_o = -(\mu-2\nu)(P/\sigma_o)/(b^2/a^2-1) \quad (44)$$

$$(E/\sigma_o)u'/r = (1-2\nu)(1+\nu)(\sigma_r'/\sigma_o) - \nu E\epsilon_z'/\sigma_o - (1-\nu^2)(\rho'/r)^2 g(\zeta_\rho') \quad (45)$$

The residual stresses and the residual displacement are found by addition

$$\sigma_r'' = \sigma_r + \sigma_r' \quad , \quad \sigma_\theta'' = \sigma_\theta + \sigma_\theta' \quad , \quad \sigma_z'' = \sigma_z + \sigma_z'$$

and

$$u'' = u + u' \quad (46)$$

## NUMERICAL RESULTS AND DISCUSSION

The numerical results for three closed-end thick-walled cylinders with various wall ratios have been obtained. The material constants in all cases were $\nu = 0.3$, $E/\sigma_o = 200$, and $m = 0.01$. The Bauschinger effect factor (f) was determined during computations based on the experimental curve $f(\epsilon^p)$ as shown in Figure 8 of Reference 9. The slope of unloading after reverse yielding was estimated to be $m' = 0.3$ for a high strength steel. The computations for the stresses, strains, and displacements during elastic-plastic loading and after complete unloading were made, and some of the numerical results are presented graphically in Figures 3 through 9.

Figure 3 shows the relation between the pressure factor and the dimensionless elastic-plastic boundary for a tube of wall ratio two. Also shown in the figure is the functional relationship between the residual displacement at the bore and the amount of overstrain. The new results for the residual displacement shown in the figure are a little smaller than the well-known results based on complete elastic unloading or the isotropic hardening model.

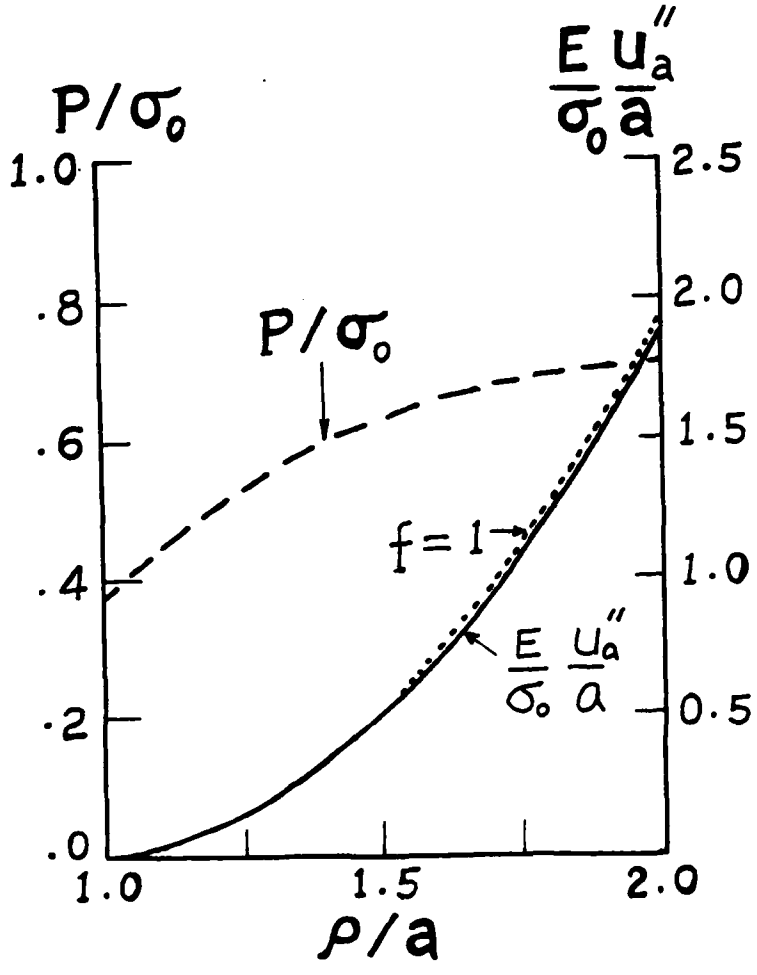


Figure 3. Internal pressure and residual displacement vs. elastic-plastic interface for the case of wall ratio two.

A similar result for a closed-end tube of wall ratio three is shown in Figure 4. The applied pressure to reach 100 percent overstrain for the case of wall ratio three is 1.61 times that for the case of wall ratio two. The residual displacement at the bore has been increased from $u_a''/a$ = 0.937 percent for the case of b/a = 2 to $u_a''/a$ = 2.939 percent for the case of b/a = 3.

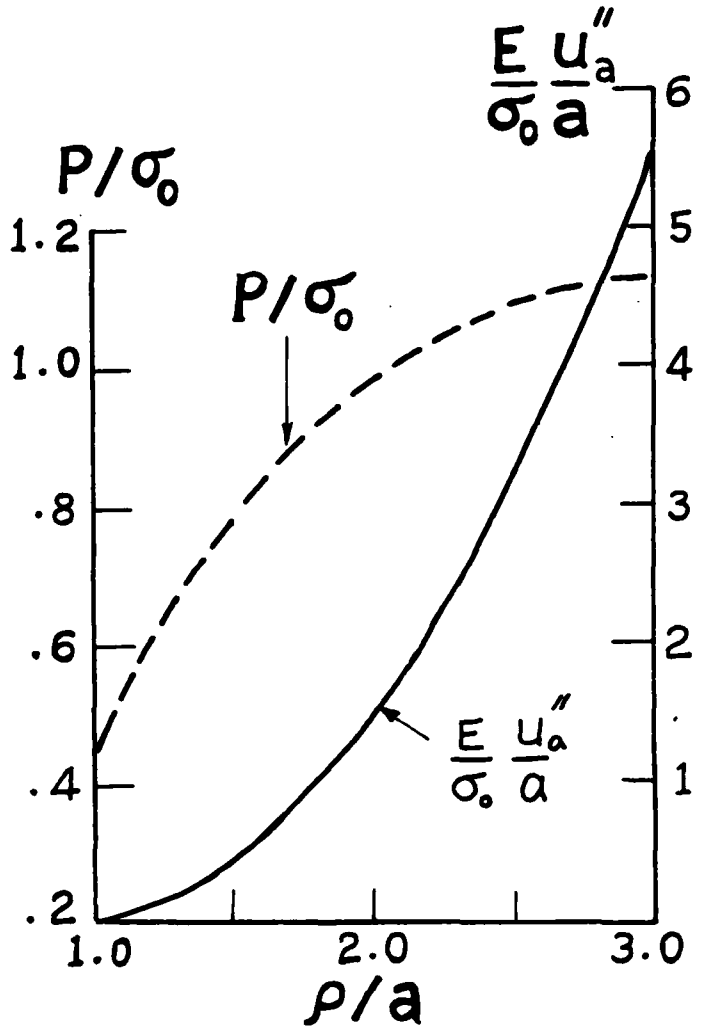


Figure 4. Internal pressure and residual displacement vs. elastic-plastic interface for the case of wall ratio three.

Since the radial and axial stresses are not as important as the hoop stress, only the numerical results for the latter are presented. Figure 5 shows the distribution of residual hoop stresses in a tube of wall ratio two subjected to 25, 50, and 75 percent overstrain. The elastic-plastic locations and the pressure factors corresponding to three cases are $\rho/a$ = 1.25, 1.50, 1.75, and $p/\sigma_0$ = 0.5284, 0.6265, 0.6818. Reverse yielding zones occur for the second and third cases, but not for the first case. Figure 6 shows the

distribution of residual hoop stresses in a closed-end tube of wall ratio three subjected to 25, 50, and 75 percent overstrain. Reverse yielding occurs for all cases and spreads a larger zone as the amount of overstrain increases.

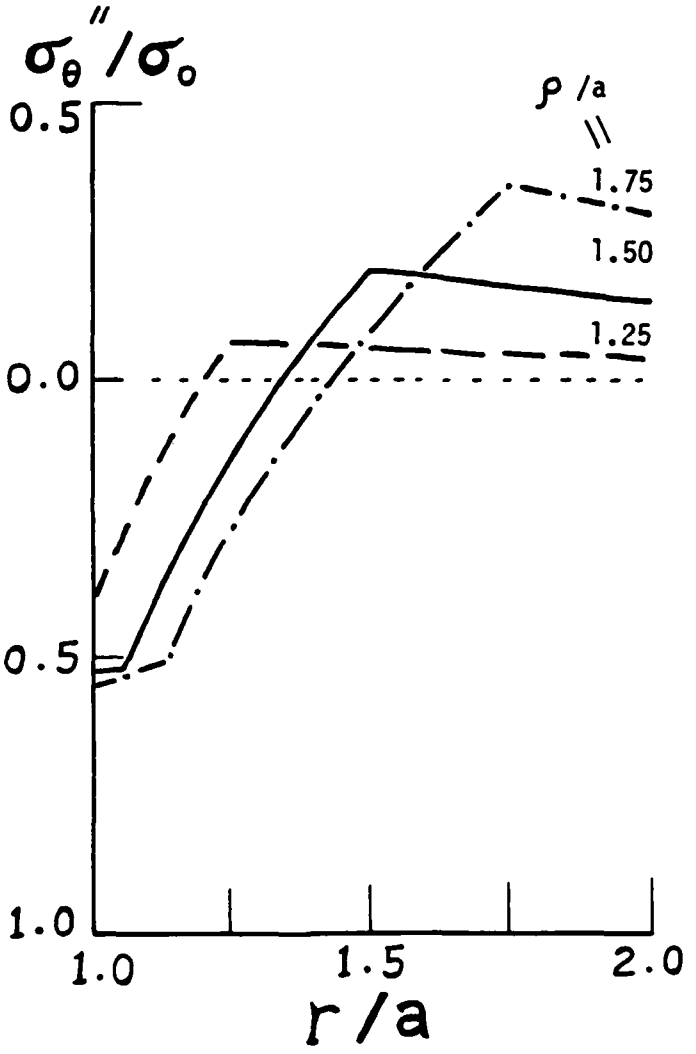


Figure 5. Residual stress distribution in an autofrettaged tube (b/a = 2.0).

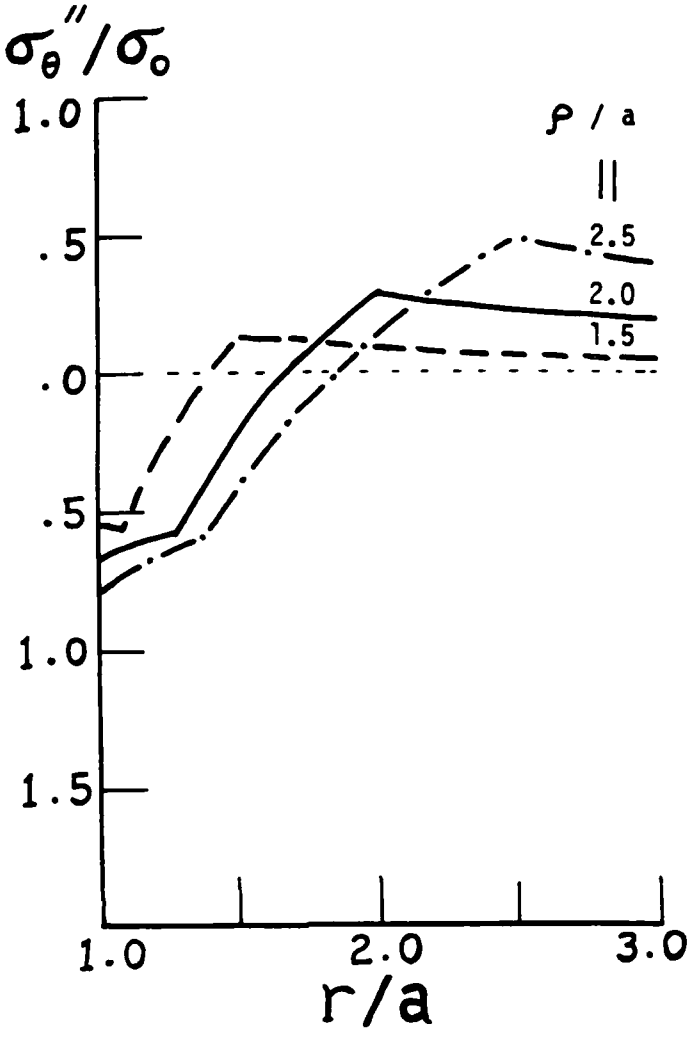


Figure 6. Residual stress distribution in an autofrettaged tube (b = 3a).

It is of interest to compare the new results for residual hoop stresses with those based on the other theoretical models. Figure 7 shows a comparison of residual hoop stresses based on three theoretical models for an autofrettaged tube of b/a = 2, $\rho$/a = 1.75. The dotted line represents the well-known solution based on the assumption of complete elastic unloading. The same solution is obtained when either the isotropic or the kinematic hardening model is used. The broken line represents the solution based on a model including the Bauschinger effect but with the same hardening parameter m' = m

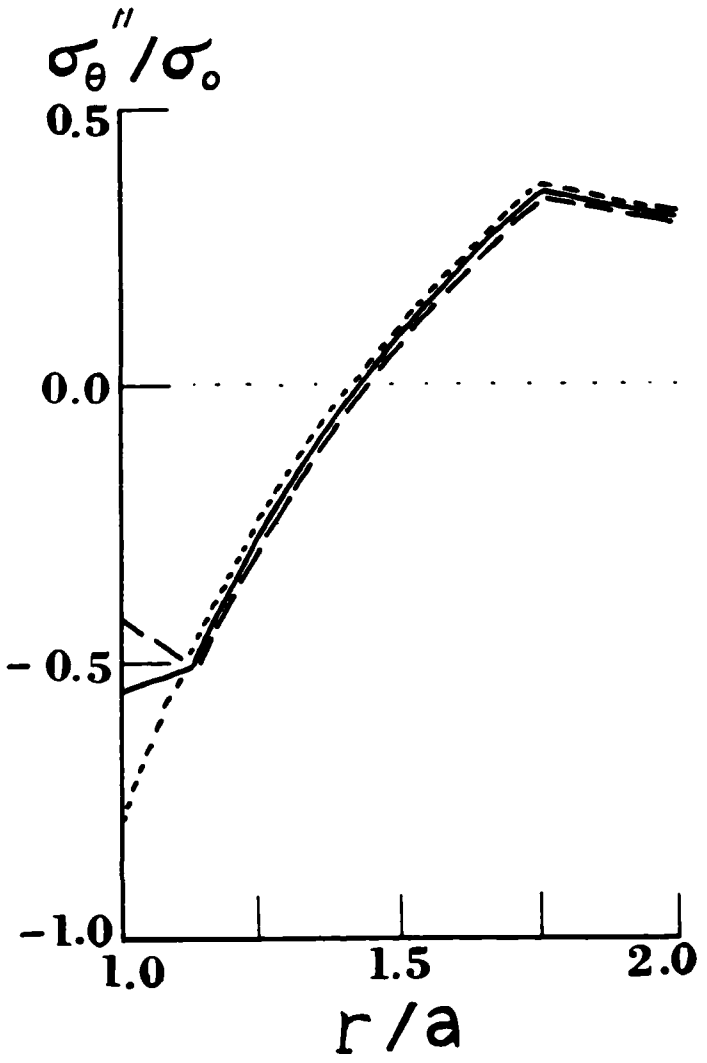


Figure 7. A comparison of residual stress based on three material models (b/a = 2, ρ/a = 1.75).

= 0.01. This solution is close to Parker's solution neglecting hardening completely with m' = m = 0 (ref 8). As can be seen from this figure, the new result represented by the solid line is quite different from the other two solutions. This comparison also demonstrates that the Bauschinger effect and strain-hardening during loading and unloading can have a significant effect on the residual stresses, especially near the bore. For a closed-end tube of wall ratio three subjected to 50 and 100 percent overstrain, we show the

comparison of residual hoop stresses based on three models in Figures 8 and 9, respectively. The dotted lines represent the solutions based on the isotropic hardening model (ref 3). Reverse yielding occurs even if the Bauschinger effect is neglected. The solid and broken lines represent the new model and the model with m' = m, respectively. As can be seen from these figures, the numerical results of the residual hoop stresses based on three models are quite different in the reverse yielding zone. The new result is considered more accurate for our problem because it is based on a more general theoretical model considering the Bauschinger and hardening effects during loading and unloading.

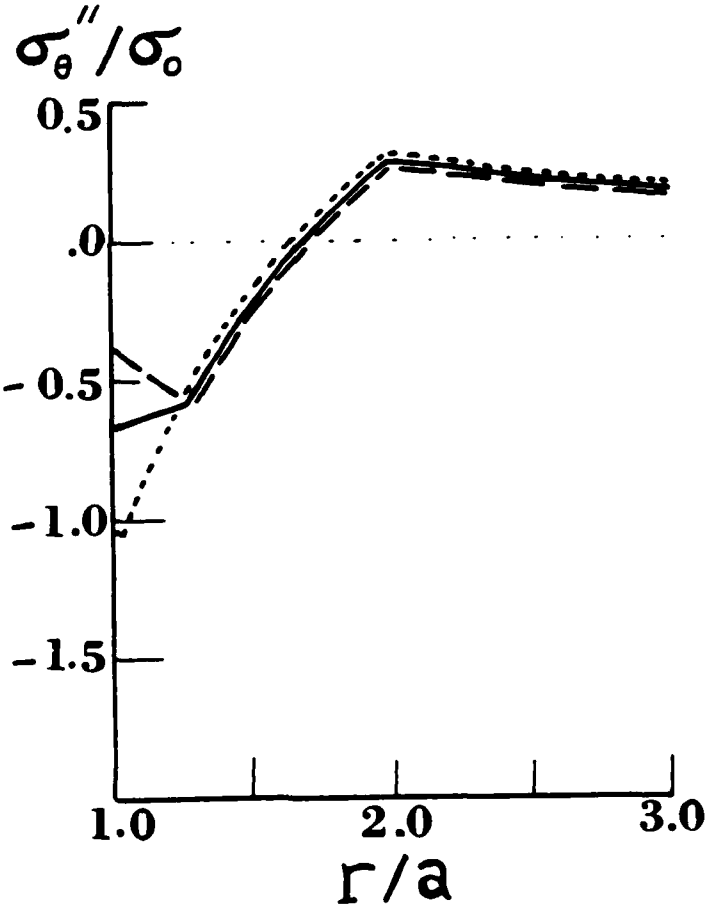


Figure 8. A comparison of residual stress based on three material models (b/a = 3, $\rho$/a = 2.0).

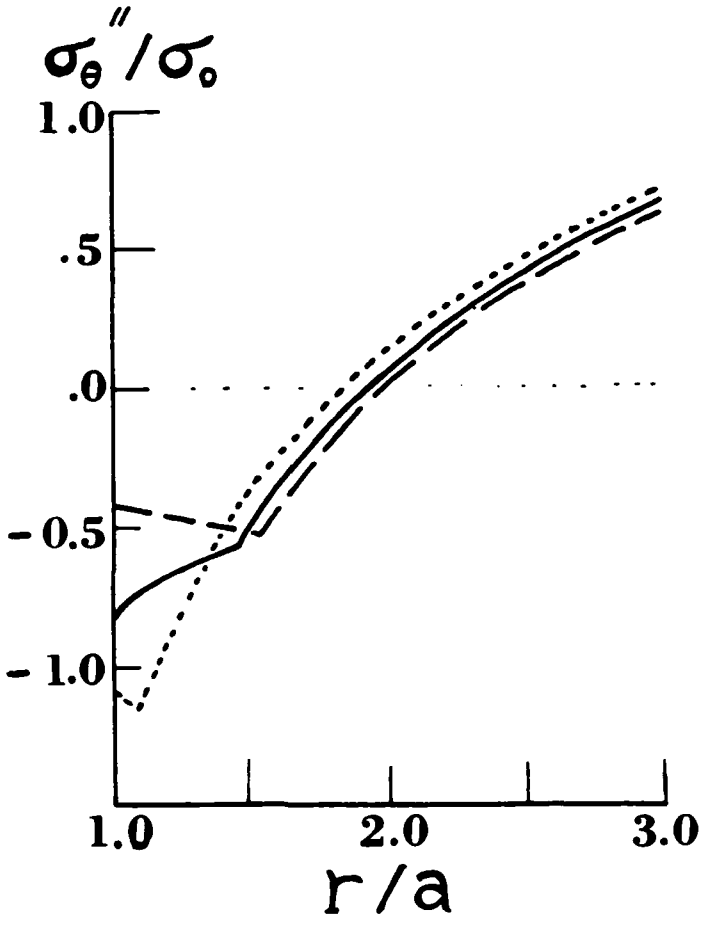


Figure 9. A comparison of residual stress based on three material models (b/a = 3, $\rho$/a = 3.0).

## REFERENCES


1. Davidson, T. E. and Kendall, D. P., "The Design of Pressure Vessels for Very High Pressure Operation," Mechanical Behavior of Materials Under Pressure, (H. L. P. Pugh, ed.), Elsevier Co., 1970.

2. Hill, R., The Mathematical Theory of Plasticity, Oxford University Press, London, 1950.

3. Bland, D. R., "Elastoplastic Thick-Walled Tubes of Work-Hardening Materials Subject to Internal and External Pressures and Temperature Gradients," Journal of Mechanics and Physics of Solids, Vol. 4, 1956, pp. 209-229.

4. Franklin, G. J. and Morrison, J. L. M., "Autofrettage of Cylinders: Prediction of Pressure/External Expansion Curves and Calculation of Residual Stresses," Proceedings of the Institute of Mechanical Engineers, Vol. 174, 1960, pp. 947-974.

5. Chen, P. C. T., "The Finite Element Analysis of Elastic-Plastic Thick-Walled Tubes," Proceedings of Army Symposium on Solid Mechanics, The Role of Mechanics in Design-Ballistic Problems, 1972, pp. 243-253.

6. Chen, P. C. T., "A Comparison of Flow and Deformation Theories in a Radially Stressed Annular Plate," Journal of Applied Mechanics, Vol. 40, 1973, pp. 283-287.

7. Chen, P. C. T., "Numerical Prediction of Residual Stresses in an Autofrettaged Tube of Compressible Material," Proceedings of the 1981 Army Numerical Analysis and Computer Conference, pp. 351-362.

8. Parker, A. P. and Andrasic, C. P., "Safe Life Design of Gun Tubes - Some Numerical Methods and Results," Proceedings of the 1981 Army Numerical Analysis and Computer Conference, pp. 311-333.

9. Milligan, R. V., Koo, W. H., and Davidson, T. E., "The Bauschinger Effect in a High Strength Steel," Journal of Basic Engineering, Vol. 88, pp. 480-488.

10. Chen, P. C. T., "The Bauschinger and Hardening Effect on Residual Stresses in an Autofrettaged Thick-Walled Cylinder," Journal of Pressure Vessel Technology, Vol. 108, February 1986, pp. 108-112.

11. Chen, P. C. T., "Prediction of Residual Stresses in an Autofrettaged Thick-Walled Cylinder," Materials Research Society Symposium Proceedings, Vol. 22, 1984, pp. 235-238.

12. Armen, H., "Plasticity in General Software," Workshop on Inelastic Constitutive Equations for Metals, (E. Krempl, C. H. Wells, and Z. Zudans, eds.), Rensselaer Polytechnic Institute, Troy, NY, 1975, pp. 56-78.

TECHN. L REPORT INTERNAL DISTRIBUTION LIST

| | NO. OF COPIES |
|---|---|
| CHIEF, DEVELOPMENT ENGINEERING BRANCH | |
| ATTN: SMCAR-CCB-D | 1 |
| -DA | 1 |
| -DP | 1 |
| -DR | 1 |
| -DS (SYSTEMS) | 1 |
| -DC | 1 |
| -DM | 1 |
| CHIEF, ENGINEERING SUPPORT BRANCH | |
| ATTN: SMCAR-CCB-S | 1 |
| -SE | 1 |
| CHIEF, RESEARCH BRANCH | |
| ATTN: SMCAR-CCB-R | 2 |
| -R (ELLEN FOGARTY) | 1 |
| -RA | 1 |
| -RM | 1 |
| -RP | 1 |
| -RT | 1 |
| TECHNICAL LIBRARY<br>ATTN: SMCAR-CCB-TL | 5 |
| TECHNICAL PUBLICATIONS & EDITING UNIT<br>ATTN: SMCAR-CCB-TL | 2 |
| DIRECTOR, OPERATIONS DIRECTORATE | 1 |
| DIRECTOR, PROCUREMENT DIRECTORATE | 1 |
| DIRECTOR, PRODUCT ASSURANCE DIRECTORATE | 1 |

NOTE: PLEASE NOTIFY DIRECTOR, BENET WEAPONS LABORATORY, ATTN: SMCAR-CCB-TL, OF ANY ADDRESS CHANGES.

TECHNICAL REPORT EXTERNAL DISTRIBUTION LIST

| | NO. OF COPIES |
|---|---|
| ASST SEC OF THE ARMY<br>RESEARCH & DEVELOPMENT<br>ATTN: DEP FOR SCI & TECH<br>THE PENTAGON<br>WASHINGTON, D.C. 20315 | 1 |
| COMMANDER<br>DEFENSE TECHNICAL INFO CENTER<br>ATTN: DTIC-DDA<br>CAMERON STATION<br>ALEXANDRIA, VA 22314 | 12 |
| COMMANDER<br>US ARMY MAT DEV & READ COMD<br>ATTN: DRCDE-SG<br>5001 EISENHOWER AVE<br>ALEXANDRIA, VA 22333 | 1 |
| COMMANDER<br>ARMAMENT RES & DEV CTR<br>US ARMY AMCCOM<br>ATTN: SMCAR-FS<br>SMCAR-FSA<br>SMCAR-FSM<br>SMCAR-FSS<br>SMCAR-AEE<br>SMCAR-AES<br>SMCAR-AET-O (PLASTECH)<br>SMCAR-MSI (STINFO)<br>DOVER, NJ 07801 | 1<br>1<br>1<br>1<br>1<br>1<br>1<br>2 |
| DIRECTOR<br>BALLISTICS RESEARCH LABORATORY<br>ATTN: AMXBR-TSB-S (STINFO)<br>ABERDEEN PROVING GROUND, MD 21005 | 1 |
| MATERIEL SYSTEMS ANALYSIS ACTV<br>ATTN: DRXSY-MP<br>ABERDEEN PROVING GROUND, MD 21005 | 1 |
| COMMANDER<br>US ARMY AMCCOM<br>ATTN: SMCAR-ESP-L<br>ROCK ISLAND, IL 61299 | 1 |
| COMMANDER<br>ROCK ISLAND ARSENAL<br>ATTN: SMCRI-ENM (MAT SCI DIV)<br>ROCK ISLAND, IL 61299 | 1 |
| DIRECTOR<br>US ARMY INDUSTRIAL BASE ENG ACTV<br>ATTN: DRXIB-M<br>ROCK ISLAND, IL 61299 | 1 |
| COMMANDER<br>US ARMY TANK-AUTMV R&D COMD<br>ATTN: TECH LIB - DRSTA-TSL<br>WARREN, MI 48090 | 1 |
| COMMANDER<br>US ARMY TANK-AUTMV COMD<br>ATTN: DRSTA-RC<br>WARREN, MI 48090 | 1 |
| COMMANDER<br>US MILITARY ACADEMY<br>ATTN: CHMN, MECH ENGR DEPT<br>WEST POINT, NY 10996 | 1 |
| US ARMY MISSILE COMD<br>REDSTONE SCIENTIFIC INFO CTR<br>ATTN: DOCUMENTS SECT, BLDG. 4484<br>REDSTONE ARSENAL, AL 35898 | 2 |
| COMMANDER<br>US ARMY FGN SCIENCE & TECH CTR<br>ATTN: DRXST-SD<br>220 7TH STREET, N.E.<br>CHARLOTTESVILLE, VA 22901 | 1 |

NOTE: PLEASE NOTIFY COMMANDER, ARMAMENT RESEARCH, DEVELOPMENT, AND ENGINEERING CENTER, US ARMY AMCCOM, ATTN: BENET WEAPONS LABORATORY, SMCAR-CCB-TL, WATERVLIET, NY 12189-4050, OF ANY ADDRESS CHANGES.

TECHNICAL REPORT EXTERNAL DISTRIBUTION LIST (CONT'D)

| | NO. OF COPIES |
|---|---|
| COMMANDER<br>US ARMY LABCOM<br>MATERIALS TECHNOLOGY LAB<br>ATTN: SLCMT-IML<br>WATERTOWN, MA 01272 | 2 |
| COMMANDER<br>US ARMY RESEARCH OFFICE<br>ATTN: CHIEF, IPO<br>P.O. BOX 12211<br>RESEARCH TRIANGLE PARK, NC 27709 | 1 |
| COMMANDER<br>US ARMY HARRY DIAMOND LAB<br>ATTN: TECH LIB<br>2800 POWDER MILL ROAD<br>ADELPHIA, MD 20783 | 1 |
| COMMANDER<br>NAVAL SURFACE WEAPONS CTR<br>ATTN: TECHNICAL LIBRARY<br>CODE X212<br>DAHLGREN, VA 22448 | 1 |
| DIRECTOR<br>US NAVAL RESEARCH LAB<br>ATTN: DIR, MECH DIV<br>CODE 26-27, (DOC LIB)<br>WASHINGTON, D.C. 20375 | 1<br>1 |
| COMMANDER<br>AIR FORCE ARMAMENT LABORATORY<br>ATTN: AFATL/DLJ<br>AFATL/DLJG<br>EGLIN AFB, FL 32542 | 1<br>1 |
| METALS & CERAMICS INFO CTR<br>BATTELLE COLUMBUS LAB<br>505 KING AVENUE<br>COLUMBUS, OH 43201 | 1 |

NOTE: PLEASE NOTIFY COMMANDER, ARMAMENT RESEARCH, DEVELOPMENT, AND ENGINEERING CENTER, US ARMY AMCCOM, ATTN: BENET WEAPONS LABORATORY, SMCAR-CCB-TL, WATERVLIET, NY 12189-4050, OF ANY ADDRESS CHANGES.

END

DTIC

9-86